Photo-physical characterization of fluorophore Ru(bpy)$_3^{2+}$ for optical biosensing applications

E.L. Sciuto [a,*], M.F. Santangelo [b], G. Villaggio [c], F. Sinatra [c], C. Bongiorno [b], G. Nicotra [b], S. Libertino [b]

[a] Material Science and Nanotechnologies, Dipartimento di Fisica e Astronomia, Univ. of Catania, Catania, Italy
[b] CNR-IMM Sede, Catania, Italy
[c] Dipartimento di Scienze Biomediche e Biotecnologiche, Catania, Italy

ABSTRACT

We studied absorption, emission and lifetime of the coordination compound tris(2,2′-bipyridyl)ruthenium(II) fluorophore (Ru(bpy)$_3^{2+}$) both dissolved in water solutions and dried. Lifetime measurements were carried out using a new detector, the Silicon Photomultiplier (SiPM), which is more sensitive and physically much smaller than conventional optical detectors, such as imager and scanner. Through these analyses and a morphological characterization with transmission electron microscopy, revealed its usability for sensor applications, in particular, as dye in optical DNA-chip technology, a viable alternative to the conventional CY5 fluorophore. The use of Ru(bpy)$_3^{2+}$ would solve some of the typical disadvantages related to Cy5's application, such as self-absorption of fluorescence and photobleaching. In addition, the Ru(bpy)$_3^{2+}$ longer lifetime may play a key role in the definition of new optical DNA-chip.

© 2015 The Authors. Published by Elsevier B.V. This is an open access article under the CC BY-NC-ND license (http://creativecommons.org/licenses/by-nc-nd/4.0/).

1. Introduction

Optical DNA-chips are widely used to study genome, gene expression, genetic diseases [1] and microbial detection [2]. We can divide the DNA-chip into three basic components: the sensing element or probe specific for target gene (single strand DNA); the labeling molecule, i.e. the conventional fluorophore CY5 (indodicarbocyanine) [3]; the optical detector, i.e. imagers or scanners. The final goal of our work is to integrate the whole biosensor system in a single portable device easy to design and fabricate. To this purpose, the first issue to address is the fluorescent labeling of the target.

For DNA labeling, the cyanine dye CY5 is conventionally used. However, it suffers of self-absorption of its fluorescence [4], caused by the proximity of absorption and emission's peaks, at 650 nm and 670 nm, respectively. At the same time, it is photobleached after prolonged exposure to laser beam (see Fig. 4B). Moreover, its short lifetime (1–3 ns) [5], would imply a quite sophisticated electronic and optical systems. Therefore, we studied an alternative fluorophore to be used in DNA-chip application, the tris(2,2′-bipyridyl)ruthenium(II) (Ru(bpy)$_3^{2+}$). It is an octahedral metal transition complex composed by the transition metal ruthenium bounded to three heteroaromatic bypiridine units. Its optical properties would allow one to overpass some issues, related to the use of CY5, as already described. The fluorophore has two absorption peaks at 290 nm and 450 nm, ligand-center (LC) and metal–ligand (MLCT) electronic transitions respectively, and a quantum yield of 0.042 ± 0.002 (compared to 0.2 of Cy5). They are far away from the emission peak at 630 nm [6,7], 100 nm the closest absorption peak, thus avoiding the fluorescence self-absorption. Therefore, the incident radiation may be shielded using a simple and inexpensive band-pass filter. Moreover, Ru(bpy)$_3^{2+}$ fluorescence exhibits a very long lifetime ($\tau = 350$ ns) [8], allowing one the use of pulsed LED for excitation.

Ru(bpy)$_3^{2+}$ has been already used in bio-sensing applications: optical environmental sensors [9]; electrical sensors, based on the electro-chemo-luminescence of Ru(bpy)$_3^{2+}$ [10]; lysozyme based optical aptasensors [11]; light switching experiments, based on direct linkage to DNA [12,13]. In this last case, the fluorophore structure was modified through the substitution of one of the bipyridyl groups with a dipyridophenazine. Thereby, fluorophore emission switched on once intercalated among base pairs of DNA double helix (especially inserted into AA mismatches).

However, there are few evidence about Ru(bpy)$_3^{2+}$ used in DNA optical sensing applications. For this reason, we studied extensively Ru(bpy)$_3^{2+}$ absorption, emission and fluorescence lifetime, focusing on its suitability to realize a portable and easy to use biosensor

* Corresponding author.
E-mail address: emanueleluigi.sciuto@imm.cnr.it (E.L. Sciuto).

device for biomedical applications (namely the DNA-chip technology). The investigation has highlighted the fluorophore sensitivity to the environment, as supported by morphological Transmission Electron Microscopy (TEM) analysis.

2. Materials and methods

Powder of tris(2,2′-bipyridyl)dichlororuthenium(II) hexahydrate was purchased from Sigma–Aldrich, while Lumiprobe provided powder of sulfo-Cyanine5 NHS ester. Phosphate buffer saline 10× solution were from Fisher Bioreagents™. The cuvettes were UV-transparent disposable cuvettes Ultra-Micro, 2×3.5 mm^2 with 10 mm optical path; the slides were coverslip glass slide 24×60 mm^2 with 0.18 mm thickness. We dissolved uranyl acetate (EMS) to give a 4% (w/v) final concentration and filtered before the use. For TEM analysis, we used formvar carbon coated nickel grids (300 mesh). The aqueous solution of Ru(bpy)$_3^{2+}$ for TEM analysis was prepared using Milli-Q ultrapure water, 18 MΩ.

We prepared tris(2,2′-bipyridyl)dichlororuthenium(II) (0.7 mg/ml) and sulfo-Cyanine5 NHS ester (0.7 mg/ml) dilutions in Milli-Q ultrapure water. We spotted 2 μl of dilutions onto glass, aluminum and silicon slides and left to dry for 30′, in a dry environment at atmospheric pressure. Then, we analyzed both the dried and the dissolved forms.

Absorption analysis were carried out using a spectrophotometer Varian Cary50. The absorption was measured for Ru(bpy)$_3^{2+}$ 0.7 mg/ml dilution in aqueous solution, inside a cuvette (dissolved form) and over a glass slide (dried form) containing 2 μl spot of solution. We chose this fluorophore concentration since the fluorescence signal is the maximum, avoiding both powder excess and optical signal saturation. For dried form absorption analysis, we collected the signal from dye spotted on glass slide fixed on solid sample holder of Cary 50.

Emission analysis were carried out on the same Ru(bpy)$_3^{2+}$ solution. Also in this case, the fluorophore was analyzed in both dissolved and dried forms. The system included: laser source (Coherent) operating at 408 nm to a power of 50 mW; chopper; monochromator; PMT Hamamatsu R-908; lock-in; a series of mirrors to collect the signal at the monochromator entrance slits. A computerized system for instruments management and data acquisition, through the software Labview®, completed the system.

Lifetime measurements on Ru(bpy)$_3^{2+}$ dissolved and dried forms were carried out by replacing the PMT with the Silicon Photomultiplier (SiPM) [5,14,15]. We placed the sample in front of the laser source. The laser was connected to a pulse generator to regulate the duration (10 ns for measurements) and frequency (50 Hz) of pulsed light. The light emitted by the sample after laser excitation reached the SiPM, located inside of a metal holed box (miniDom [16]) which also contained some electrical high-pass filters. A computer collected the SiPM detection signal, measured by a source-meter-unit (Keithley 236). Finally, an optical band-pass filter at 600 ± 30 nm was placed within the miniDom, to exclude the excitation beam.

In order to study its photostability, we measured Ru(bpy)$_3^{2+}$ absorption and emission under very unsustainable chemical-physical conditions (see Supplemental materials).

Finally, transmission electron microscopy (TEM) experiments were performed using the bright field in conventional parallel beam (CTEM) mode (BF). A TEM JEOL JEM-2010 equipped with a 30 mm^2 window energy dispersive X-rays (EDX) spectrometer was used. Ru(bpy)$_3^{2+}$ was examined by negative contrast according to the following protocol. A mix of 8 μl of 4% uranyl acetate, used as contrast element, and 12 μl of 0.7 mg/ml fluorophore dilution was prepared. Subsequently, 20 μl of the mix were placed on the formvar carbon coated nickel grid and the excess was removed by a filter paper. After drying for 10′ at room temperature, we examined samples inside the microscope.

3. Results and discussion

Absorption data for Ru(bpy)$_3^{2+}$ dissolved and dried form are shown in Fig. 1. The data obtained from the dissolved form (blue solid line) perfectly reproduce literature results [6,7]. The fluorophore exhibits two characteristic absorption peaks at 290 nm and 450 nm (highlighted in figure with dashed vertical lines). On the other hand, samples dried over glass slides showed a red shift of about 20 nm, with electronic transition's peaks at 310 nm and 470 nm, as shown in Fig. 1 (red dashed line). The absorption "red shift" is probably due either to the intensification of inter-molecular interactions or to a slight distortion of the intra-molecular bonds. Actually, drying process generates the increase of fluorophore's molecular density and, accordingly, a structural compression and deformation. The result could be an alteration of standard intramolecular electronic transitions and absorption peaks. The data,
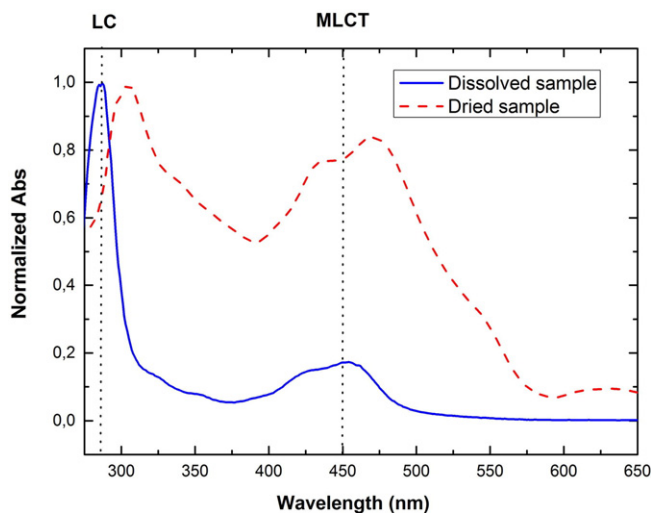

Fig. 1. Absorption spectra of dissolved (blue solid line) and dried (red dashed line) form of Ru(bpy)$_3^{2+}$; the ligand-center (LC) and metal–ligand (MLCT) electronic transitions are highlighted with vertical dashed lines.
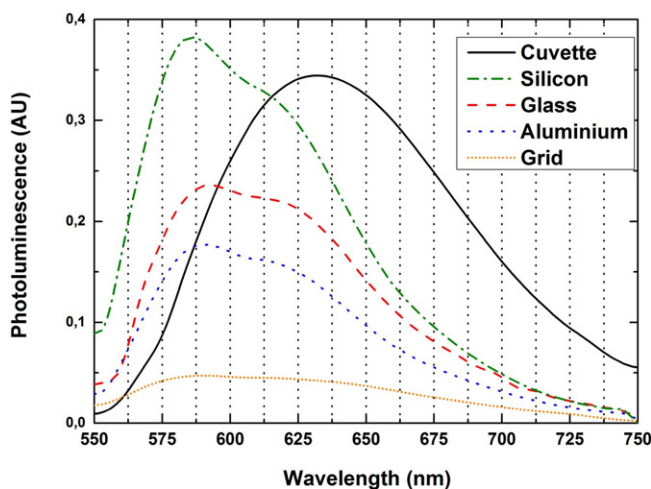

Fig. 2. Ru(bpy)$_3^{2+}$ emission spectra dissolved in water (black curve) or deposited on: silicon (green dot-dashed line), glass (red dashed line), aluminum (blue dotted line) and C grid for microscopy (orange points).
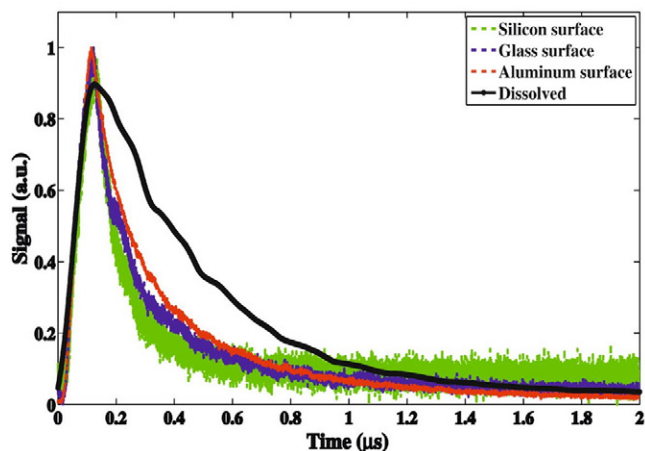
Fig. 3. Lifetime of dissolved (black line) and dried (blue, green and red lines) forms of $Ru(bpy)_3^{2+}$.

shown in Fig. 1, clearly show a difference in the ratio between LC and MLCT transitions. The MLCT–LC ratio goes from ~0.2 of the dissolved form to more than 0.8 of the dried form, suggesting a strong increase of the absorption efficiency, more than a factor four, of the MLCT electronic transitions with respect to the LC ones.

The emission spectrum of the 0.7 mg/ml sample in cuvette is shown in Fig. 2 (black solid line). The curve perfectly mirrors the literature emission spectra, exhibiting a peak at about 630 nm [6].

Quite different is the case of the fluorophore dried form. The emission spectra are, for such form, quite different from literature data [7]. The curve morphology changed and a new and dominant peak around 590 nm appeared (red line in Fig. 2). In order to exclude any contribution given by the solid surface used for deposition, we spotted $Ru(bpy)_3^{2+}$ on aluminum (Al), silicon (Si), and glass surfaces as well as on the grids used for TEM analysis (see experimental). The emission data are also shown in Fig. 2 (blue, green and orange line, respectively): they exhibit the same morphological alteration of the curve (the new dominant peak at 590 nm) already observed for the dried sample on glass slide, only the relative height are different, but no conclusion can be drown from the PL intensity at room temperature. It should be underlined we used an insulator (glass), semiconductor (Si, to be sure that the surface was Si, a sample deep in HF was performed just before fluorophore deposition), metal (Al) and C coated grids as deposition surfaces. The goal was to determine if the surface electronic properties could modify the fluorophore emission properties. The data clearly show that the surface role is not the dominant effect ruling the $Ru(bpy)_3^{2+}$ emission properties, at the deposition conditions used.

We believe that the strong blue shift of the emission peak is due to a cooperative interaction of the molecules, as already observed in the absorption measurements. In fact, the shift may be attributed to a HOMO (highest occupied molecular orbital) – LUMO (lowest unoccupied molecular orbital) distance shift. According to literature [8], such shift could be originated by a strong interaction with the substrate, as we observed analyzing dried Cy5 emission. Cy5 showed different peaks and emission curves depending of which type of surface (insulating or not) is used for spotting (see Fig. 1 in Supplemental materials). In Cy5 the stabilization of the HOMO orbital, which could cause the shift of the emission peak, is given by the insulating substrate presence. For dried $Ru(bpy)_3^{2+}$, instead, we believe that the stabilizing interaction occurs not with the substrate but among the molecules themselves. Two main evidences allow us to support such conclusion. First, in Ref. [8], the substrate was powdered and mixed to the fluorophore in order to enhance the interaction. The full mix was dried. In our case the solution is just spotted on the substrate, hence, the interaction with the substrate is only due to the molecular layer at the interface and many layer are deposited on top of it. Second, in our case the emission blue shift occurs regardless of the substrate characteristics. The same peak occurs if the fluorophore is deposited on an insulator (glass), a semiconductor (Si) or a conductor (Al) surface. The only difference being the peak intensity. We believe in our experimental set-up, is the molecule-to-molecule interaction to dominate the emission properties, suggesting the molecules, if available in a suitable concentration, tend to interact, even clustering.

The last optical characterization was the $Ru(bpy)_3^{2+}$ lifetime using a SiPM detector. As already observed for the emission, the lifetime value changed depending on the fluorophore physical state (dissolved or dried), as shown in Fig. 3. The experimental data (points in figure) were fitted (dashed red lines) to obtain the lifetime (τ) values. To perform the analysis we used a multi-exponential as indicated by the following equation:

$$F(t) = \sum_i A_i \cdot \exp(-t/\tau_i) \qquad (1)$$

The lifetime measured in solution (0.7 mg/ml of fluorophore in Milli-Q water) was 358 ± 0.9 ns (see Fig. 3 black line and Table 1), according to literature [8], within the experimental errors. To validate SiPM and whole experimental system's efficiency we measured also Cy5's lifetime, which was 2.15 ± 0.06 ns as reported in other works [5] (see Table 1).
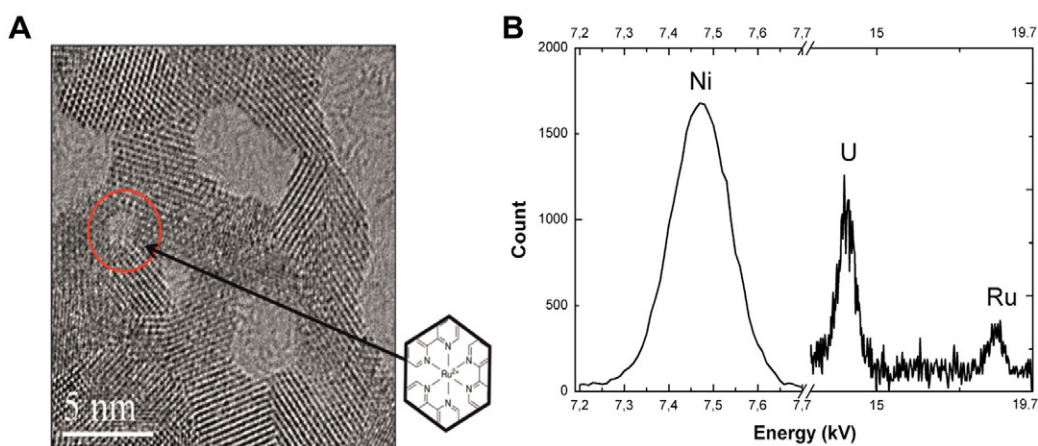

Fig. 4. (A) HRTEM image of $Ru(bpy)_3^{2+}$ clusters; red circle highlights the supposed fluorophore's single molecule. (B) EDX spectrum of TEM grid containing nickel (Ni) and the mix of $Ru(bpy)_3^{2+}$ (Ru) and uranyl acetate (U).

Table 1
Lifetime values.

Sample [a]	τ_1	τ_2
Cy5 dissolved	2.15 ± 0.06 ns	–
$Ru(bpy)_3^{2+}$ dissolved		358 ± 0.9 ns
$Ru(bpy)_3^{2+}$ dried on glass	118 ± 1 ns	358 ns
$Ru(bpy)_3^{2+}$ dried on silicon	130 ± 3 ns	372 ± 49 ns
$Ru(bpy)_3^{2+}$ dried on aluminum	130 ± 3 ns	370 ± 3 ns

[a] All samples were diluted in Milli-Q water.

For $Ru(bpy)_3^{2+}$ dried samples, the lifetime was given by two components. These data confirmed that the fluorophore interactions modified the fluorescent properties; in fact, we observed a second emission peak with a shorter lifetime. The lifetime was measured for all the surfaces used to deposit the fluorophore: glass, Si and Al. The data, shown in Fig. 3, are also summarized in Table 1. In the table are reported three lifetime values to make easier the comparison. In fact, all the samples exhibit the τ_2 component, typical of the suspended form. The strong difference observed is $Ru(bpy)_3^{2+}$ deposited on both glass and Al, an insulator and a conductor surface, respectively, exhibit a shorter lifetime component.

In all measurements, the lifetime is always over 100 ns, a promising feature for our applications.

All results here reported show that $Ru(bpy)_3^{2+}$ has biochemical and optical properties useful for target gene labeling in miniaturized DNA-chip. In fact, the fluorophore emission peak is far away from the absorption one. It makes possible to avoid the self-quenching. $Ru(bpy)_3^{2+}$ exhibits a quite long lifetime, which would allow us to use a simple electronic system to drive the source and detectors in an integrated DNA-chip. Moreover, it is photostable, as shown in Fig. 2 of Supplemental materials.

In literature, there are some evidences about spotted surface effects on photochemical properties of $Ru(bpy)_3^{2+}$, in terms of structural sensitivity to O_2 [17] and "rigidochromism" [18] if fluorophore is encapsulated in polymers. However, the optical characterization we performed, clearly indicated a $Ru(bpy)_3^{2+}$ sensitivity to its physical state and environment, independently from the surface. Its excitation/emission properties changes with the state transition from dissolved to dried form, probably due to molecule–molecule aggregations, rather than surface-molecule interaction. This hypothesis was verified by a careful study using TEM analysis.

We used TEM microscopy to observe the fluorophore molecules in dried form, in order to verify if the absorption/emission changes of $Ru(bpy)_3^{2+}$ could be related to molecular cooperation. Like many carbon based molecules, even the $Ru(bpy)_3^{2+}$ is very sensitive to the electron beam and very light to have a high contrast on the image. In order to identify and study the fluorophore dried steric conditions, we performed a phase contrast imaging with the HRTEM. The analysis clearly showed a thin crystalline layer coming from the negative contrast element (uranyl acetate) deposited on the TEM grid, as shown by the image in Fig. 4A. This layer surrounds regions having a different contrast. Chemical analysis through EDX spectroscopy (reported in Fig. 4B) confirmed that within these regions there was ruthenium, unlike in the rest of the grid.

These results allowed us to conclude that $Ru(bpy)_3^{2+}$ in dried form may collapse in clusters but a certain percentage of single molecules is also visible. See, as an example, the impressive image (within the red circle) showing the crystallographic planes of uranyl acetate arranged around a region perfectly resembling the $Ru(bpy)_3^{2+}$ features. Both the hexagonal geometry and the diameter (1 nm) resemble the fluorophore single molecule. The presence of lattice fringes in correspondence of the region occupied by the $Ru(bpy)_3^{2+}$, however, is a defocus artifacts that can arise from phase contrast imaging from the neighborhood uranium atoms. Wider regions surrounded by the acetate are also visible in Fig. 4A, suggesting that the molecules can agglomerate and may

interact, probably causing the small changes of their fluorescent properties previously detected.

4. Conclusion

Photochemical properties of metal transition complex tris(2,2′-bipyridyl)ruthenium(II), for optical sensing application, have been studied. The analysis showed that this molecule is a viable alternative to the conventional fluorophore CY5 for target gene labeling in optical DNA-chip. In fact, $Ru(bpy)_3^{2+}$ excludes the risk of fluorescence self-absorption, thanks to the large distance between the absorption/emission peaks, and allows the use of simple electronics for the fluorescence analysis, thanks to the long lifetime. At the same time, optical studies revealed a dependence of both fluorophore properties, emission and lifetime, on the environmental conditions. Finally, $Ru(bpy)_3^{2+}$ is photostable unlike Cy5.

The measurements showed a cooperative effect of the molecules by increasing their density during drying of sample. This caused the red shift of the absorption peaks at 310 nm and 470 nm and the appearance of a dominant emission peak at 590 nm in dried samples. These samples exhibit an additional faster component in the lifetime, in addition to the 350 ns lifetime value of dissolved samples. Furthermore, TEM analysis revealed regions with few molecules (clusters) of $Ru(bpy)_3^{2+}$ in dried form. This result lead us to suppose that, inside the clusters, the molecules of $Ru(bpy)_3^{2+}$ interact each other modifying their structure and their inner electronic transitions. This feature could explain the alteration of dried $Ru(bpy)_3^{2+}$ fluorescent properties. Further experiments are in progress to understand better this phenomenon and its usefulness for optical DNA-chip application. In fact, the dependence of $Ru(bpy)_3^{2+}$ optical characteristics on the physical state could allow the fabrication of innovative "steric condition sensitive" optical sensors.

Appendix A. Supplementary data

Supplementary data associated with this article can be found, in the online version, at http://dx.doi.org/10.1016/j.sbsr.2015.09.003.

References

[1] B. Foglieni, A. Brisci, F. San Biagio, P. Di Pietro, S. Petralia, S. Conoci, M. Ferrari, L. Cremonesi, Integrated PCR amplification and detection processes on a Lab-on-Chip platform: a new advanced solution for molecular diagnostics, Clin. Chem. Lab. Med. 48 (3) (2010) 329–336.

[2] R.W. Ye, T. Wang, L. Bedzyk, K.M. Croker, Applications of DNA microarrays in microbial systems, J. Microbiol. Methods 47–257 (2001).

[3] M. Schena, D. Shalon, R.W. Davis, P.O. Brown, Quantitative monitoring of gene expression patterns with a complementary DNA microarray, Science 270 (1995) 467–470.

[4] J.R. Lakowicz, Radiative decay engineering: biophysical and biomedical applications, Rev. Anal. Biochem. 298 (2001) 1–24.

[5] M.F. Santangelo, R. Pagano, S. Lombardo, E.L. Sciuto, D. Sanfilippo, G. Fallica, F. Sinatra, A.C. Busacca, S. Libertino, "SiPM as novel Optical Biosensor: transduction and applications", Photonics Technologies, 2014 Fotonica AEIT Italian Conference, pp. 1–4, ISBN: 978-8-8872-3718-4, Naples, 12-14 May 2014.

[6] J.N. Demas, B.A. DeGraff, Design and applications of higly luminescent transition metal complexes, Anal. Chem. 63 (1991) 829A–837A.

[7] K. Kalyanasundaram, Photophysics, photochemistry and solar energy conversion with tris(bipyridyl)ruthenium(II) and its analogues, Coord. Chem. Rev. 46 (1982) 159–244.

[8] T. Kajiwara, K. Haslmoto, T. Kawai, T. Sakata, Dynamics of luminescence from $Ru(bpy)_3Cl_2$ adsorbed on semiconductor surfaces, J. Phys. Chem. 86 (1982) 4516–4522.

[9] J.N. Demas, B.A. DeGraff, Applications of luminescent transition metal complexes to sensor technology and molecular probes, J. Chem. Ed. 74 (1997) 690–695.

[10] T.G. Drummond, M.G. Hill, J.K. Barton, Electrochemical DNA sensors, Nat. Biotechnol. 21 (2003) 1192–1199.

[11] Y. Li, H. Qi, Q. Gao, C. Zhang, Label-free and sensitive electrogenerated chemiluminescence aptasensor for the determination of lysozyme, Biosens. Bioelectron. 26 (2011) 2733–2736.

[12] A.E. Friedman, J.C. Chambron, J.P. Sauvage, N.J. Turro, J.K. Barton, A molecular light switch for DNA: Ru(bpy)$_2$(dppz)$^{2+}$, J. Am. Chem. Soc. 11 (2) (1990) 4960–4962.

[13] H. Song, J.T. Kaiser, J.K. Barton, Crystal structure of Δ-[Ru(bpy)$_2$d ppz]$^{2+}$ bound to mismatched DNA reveals side-by-side metalloinsertion and intercalation, Nat. Chem. 4 (2012) 615–620.

[14] R. Pagano, G. Valvo, D. Sanfilippo, S. Libertino, D. Corso, P.G. Fallica, S. Lombardo, Silicon photomultiplier device architecture with dark current improved to the ultimate physical limit, Appl. Phys. Lett. 102 (2013) 183502.

[15] S. Libertino, S. Conoci, M.F. Santangelo, R. Pagano, E.L. Sciuto, F. Sinatra, D. Sanfilippo, G. Fallica, S. Lombardo, Optical and electrical Si-based biosensors: fabrication and trasduction issues, J. Anal. Bioanal. Tech. S12 (2014) 007, http://dx.doi.org/10.4172/2155-9872.S12-007.

[16] S. Libertino, D. Corso, M. Lisiansky, Y. Roizin, F. Palumbo, F. Principato, C. Pace, P. Finocchiaro, S. Lombardo, Ionizing radiation effects on non volatile read only memory cells, IEEE Trans. Nucl. Sci. 59 (6) (2012) 3016.

[17] Z.J. Fuller, W.D. Bare, K.A. Kneas, W.-Y. Xu, J.N. Demas, B.A. DeGraff, Photostability of luminescent ruthenium(II) complexes in polymers and in solution, Anal. Chem. 75 (2003) 2670–2677.

[18] W.R. Glomm, S. Volden, J. Sjöblom, M. Lindgren, Photophysical properties of ruthenium(II) tris(2,2′-bipyridine) and europium(III) hexahydrate salts assembled into sol–gel materials, Chem. Mater. 17 (22) (2005) 5512–5520.